Published OnlineFirst February 10, 2009; DOI: 10.1158/0008-5472.CAN-08-3255

Research Article

Selective Inhibition of Matrix Metalloproteinase-14 Blocks Tumor Growth, Invasion, and Angiogenesis

Laetitia Devy,[1] Lili Huang,[1] Laurent Naa,[2] Niranjan Yanamandra,[1] Henk Pieters,[2] Nicolas Frans,[2] Edward Chang,[1] Qingfeng Tao,[1] Marc Vanhove,[2] Annabelle Lejeune,[2] Reinoud van Gool,[2] Daniel J. Sexton,[1] Guannan Kuang,[1] Douglas Rank,[1] Shannon Hogan,[1] Csaba Pazmany,[1] Yu Lu Ma,[1] Sonia Schoonbroodt,[2] Andrew E. Nixon,[1] Robert C. Ladner,[1] Rene Hoet,[2] Paula Henderikx,[2] Chris TenHoor,[1] Shafaat A. Rabbani,[3] Maria Luisa Valentino,[3] Clive R. Wood,[1] and Daniel T. Dransfield[1]

[1]Dyax Corp., Cambridge, Massachusetts; [2]Dyax S.A., Liege, Belgium; and [3]Department of Medicine, McGill University Health Centre, Montreal, Quebec, Canada

Abstract

Inhibition of specific matrix metalloproteinases (MMP) is an attractive noncytotoxic approach to cancer therapy. MMP-14, a membrane-bound zinc endopeptidase, has been proposed to play a central role in tumor growth, invasion, and neovascularization. Besides cleaving matrix proteins, MMP-14 activates proMMP-2 leading to an amplification of pericellular proteolytic activity. To examine the contribution of MMP-14 to tumor growth and angiogenesis, we used DX-2400, a highly selective fully human MMP-14 inhibitory antibody discovered using phage display technology. DX-2400 blocked proMMP-2 processing on tumor and endothelial cells, inhibited angiogenesis, and slowed tumor progression and formation of metastatic lesions. The combination of potency, selectivity, and robust *in vivo* activity shows the potential of a selective MMP-14 inhibitor for the treatment of solid tumors. [Cancer Res 2009;69(4):1517–26]

Introduction

Matrix metalloproteinase (MMP)-14 (MT1-MMP) is a membrane-bound MMP that plays a critical role in conferring cells with the ability to remodel and penetrate extracellular matrix (1). MMP-14 drives invasion by functioning as a pericellular collagenase (2) and an activator of proMMP-2 (3, 4), and is directly linked to tumorigenesis and metastasis (5–7). MMP-14 null mice display impaired basic fibroblast growth factor–mediated corneal angiogenesis (4), and tissues from the same mice fail to show angiogenesis in a type I collagen *ex vivo* model, supporting a potential role of MMP-14 in angiogenesis as well (8).

High MMP-14 expression is associated with early death of breast cancer patients (9) and is correlated with lymph node metastases, progression, invasion, poor clinical stage, larger tumor size, and increasing tumor stage (10, 11). Taken together with the multiple lines of preclinical evidence linking MMP-14 to cancer progression, there is a strong case for targeting MMP-14 in cancer.

Inhibition of MMPs has been extensively pursued as a therapeutic strategy for treating cancer, generally using compounds containing zinc-chelating groups such as hydroxamates. MMP intervention strategies have met with limited clinical success with severe toxicities (12, 13) in that prolonged treatment with broad-spectrum MMP inhibitors caused musculoskeletal pain and inflammation (14, 15). The mechanism of these toxicities is assumed to be due to the poor selectivity of these compounds. It is now recognized that among the MMP family, some possess cancer-promoting activities whereas others have tumor-inhibiting functions (16), underlining the risk of using broad-spectrum MMP inhibitors. In fact, broad-spectrum MMP inhibitors promote metastasis of breast carcinomas as well as lymphomas to the liver in mice (17, 18).

High selectivity is essential for realizing the clinical potential of MMP inhibitors. Using a human Fab displaying phage library, we have identified a potent and highly selective inhibitor of MMP-14, providing us with the opportunity to assess the preclinical pharmacology of this MMP inhibitor.

Materials and Methods

Phage Display Library Selections and Screenings

MMP-14 catalytic domain (MMP-14-CD; R&D Systems) was biotinylated using the EZ-Link Sulfo-NHS-LC-Biotin reagent (Thermo Fisher Scientific) and used as the target for selection against our human Fab library FAB310. Selections and Fab-phage ELISA were carried out essentially as described (19). Fabs were reformatted into whole human IgG1s (hIgG1) as described previously (20). DX-2400 was stably expressed in Chinese Hamster Ovary cells and purified using protein A, a 15S resin, and MEP HyperCell mixed mode resin (PALL Life Science). The percent aggregation was <5% and contaminants including protein A, dsDNA, host cell proteins, and endotoxins were below detectable limits.

MMP Inhibition Assays

DX-2400 was tested for MMP-14 inhibitory activity using a fluorescent peptide substrate Mca-Lys-Pro-Leu-Gly-Leu-Dap(Dnp)-Ala-Arg-NH_2 (M-2350, Bachem). The proform of the mouse, rat, and cynomolgus monkey MMP-14 without the cytoplasmic and transmembrane domains were cloned, expressed in insect cells, and purified.

K_i and apparent K_is ($K_{i\ app}$) were computed from inhibition curves (initial velocities versus DX-2400 concentrations) at different substrate concentrations (5–50 μmol/L) using the Morrison equation (21). The K_i values were calculated from $K_{i\ app}$ versus substrate concentration ($[S]$) curves and the competitive relationship between $K_{i\ app}$ and $[S]$ [$K_{i\ app} = (1 + \frac{[S]}{K_m})$] (22).

Note: Supplementary data for this article are available at Cancer Research OnLine (http://cancerres.aacrjournals.org/).

Requests for reprints: Laetitia Devy, Dyax Corp., 300 Technology Square, Cambridge, MA 02139. Phone: 617-250-5531; Fax: 617-225-2501; E-mail: ldevy@dyax.com.

doi:10.1158/0008-5472.CAN-08-3255

Published OnlineFirst February 10, 2009; DOI: 10.1158/0008-5472.CAN-08-3255

The inhibitory activities of anti–MMP-14 Fabs and IgG1s toward other human MMPs and tumor necrosis factor-α converting enzyme (TACE) were examined. MMP and TACE enzymatic activities were monitored using enzyme-specific peptide substrates in the absence or presence of 1 to 10 μmol/L anti–MMP-14 IgG1κ antibodies. Two broad-spectrum MMP inhibitors, GM6001 (Millipore Corp.) and Marimastat (Tocris Biosciences), were used as controls.

Cell-Based Assays and Gelatin Zymography

Cell culture. HT-1080, MDA-MB-231, and BT-474 cells were obtained from American Type Culture Collection and cultured according to the vendor's guidelines. MDA-MB-231 cells transfected with plasmid encoding green fluorescent protein (MDA-MB-231-GFP) were maintained in culture as described (23). Human umbilical vein endothelial cells (HUVEC) were freshly isolated from umbilical cords and cultured on gelatin-coated culture dishes in RPMI 1640 with 25 mmol/L HEPES supplemented with EGM SingleQuots (Cambrex Bio Science), 200 mmol/L L-glutamine, 1% penicillin-streptomycin, and 10% FCS. For some experiments, HUVECs were purchased from Lonza. HUVECs were used between passages 3 and 6.

Western blot analysis. Whole cell protein extracts were prepared from cells using radioimmunoprecipitation assay buffer. Equal amount of proteins (30 μg) was resolved by 4% to 12% SDS-PAGE and electroblotted onto a polyvinylidene difluoride membrane. The blot was probed with a rabbit polyclonal antibody to MMP-14 (Abcam) followed by a horseradish peroxidase (HRP)–conjugated goat anti-rabbit antibody (Thermo Fisher Scientific). Proteins were detected using a SuperSignal West Femto Maximum Sensitivity Substrate (Thermo Fisher Scientific). The blot was subsequently stripped and reprobed with a mouse monoclonal antibody to β-actin (Abcam) followed by a HRP-conjugated goat anti-mouse antibody (Thermo Fisher Scientific). For immunoprecipitation, an equal amount of cell lysates (1 mg) was incubated with 5 μL of anti–MMP-14 antibody and 20 μL of protein G beads (GE Healthcare) overnight at 4°C. After washing, beads were resuspended in sample buffer and subjected to Western blotting as described above except that a mouse anti–MMP-14 antibody (R&D Systems) was used as the primary antibody.

Gelatin zymography. HT-1080 cells (2×10^5) and HUVECs (2×10^5) were grown for 24 h in complete medium. After two washings in PBS, HT-1080 cells were treated with a broad range of DX-2400 concentrations, GM6001 (10 μmol/L), or a nonneutralizing polyclonal anti–MMP-14 antibody (R&D Systems; 67 nmol/L). Conditioned medium from HT-1080 cells was collected after 48 h of culture in serum-free UltraCulture medium (Cambrex Bio Science). After 4 h of starvation in EBM-2 basal medium, HUVECs were stimulated with vascular endothelial growth factor (VEGF)-165 (10 ng/mL) and either control IgG1 antibody (6.7 nmol/L) or DX-2400 (6.7 nmol/L). Conditioned medium was collected after 16 h of culture, and gelatinolytic activities in 10-fold concentrated conditioned media (Centricon YM-30 columns, Millipore) were analyzed by gelatin zymography (24).

Chemoinvasion assays. *In vitro* invasive properties of HUVECs were assessed using polycarbonate filters with 8 μm pore size, coated with growth factor–depleted Matrigel (BD Biosciences). HUVECs were serum starved for 4 h in EBM-2 basal media and washed twice in PBS containing 0.1% bovine serum albumin (BSA). The upper part of the chamber was filled with HUVECs (5×10^4) treated with either DX-2400 (6.7 nmol/L) or control IgG1 (6.7 nmol/L) in EBM-2 basal medium. The bottom part of the chamber was filled with EBM-2 medium supplemented with either 0.5% serum (control) or 0.5% serum with VEGF (10 ng/mL) along with control IgG1 (6.7 nmol/L) or DX-2400 (6.7 nmol/L). Anti-VEGF antibody (R&D Systems; 6.7 nmol/L) was used as a positive control. After 18 to 22 h of incubation at 37°C, invasive cells were stained with DiffQuick staining solution (Thermo Fisher Scientific) and filters were mounted onto glass slides. The number of cells that had migrated per membrane from three random fields was counted using a brightfield microscope connected to a Spot digital camera (Diagnostic Instruments).

Tube formation assay. HUVECs were seeded at a density of 2×10^4 per well on the top of a Matrigel layer according to the manufacturer's guidelines (BD Labware). Culture medium was added to each well in the presence or absence of a dose range of DX-2400. Suramin (Calbiochem) was used as a positive control. Cells were incubated at 37°C with 5% CO_2 in a humidified incubator for 16 to 18 h. Total tube length in the photomicrograph was quantified using angiogenesis tube formation application module in Metamorph software (Molecular Devices). Tube formation of untreated HUVECs was used as a negative control. The assay was done twice in triplicate with IC_{50} values determined using SigmaPlot 8.0.

Fibrin gel bead assay. Fibrin gel bead assay was done as described (25). Briefly, HUVECs were mixed with dextran-coated cytodex-2 microcarriers (Amersham Pharmacia Biotech) and treated with control IgG1 or DX-2400 for 4 h. The coated beads were then embedded in a fibrin clot and incubated with EBM-2 complete medium in the presence or absence of indicated concentrations of control IgG1 (67 nmol/L) and DX-2400 (0.67, 6.7, and 67 nmol/L). Anti-VEGF antibody (67 nmol/L) was used as a positive control. Medium and treatment were renewed every other day. After 7 d, beads were fixed and photographed. The migration distance was calculated for three random areas per bead, and data were represented as an average of eight beads. The migration distance was normalized to percent migration, with migration to control alone representing 100%.

Xenograft Models

Detailed protocols are described in Supplemental Data and Supplementary Table S1.

Analyses of the presence of GFP-positive cells in ectopic organs. Fresh lung and liver tissues were cut (1 mm thick) for direct examination by fluorescent microscopy for the presence of GFP-expressing tumor foci. The number of foci per field of examination was counted from 10 random sites of five different slides for each organ.

Evaluation of DX-2400 concentration in mouse serum. DX-2400 concentrations in mouse serum were measured using an electrochemical luminescent binding assay. Streptavidin-coated plates were used to capture biotinylated rabbit anti–DX-2400 antibody. DX-2400 standard and blinded serum samples were incubated with the coated plate at a minimum required dilution of 1:80. Unbound DX-2400 was washed off and bound DX-2400 was detected with ruthenylated rabbit anti–DX-2400 antibody. The detection limits using this assay ranged from 125 to 8,000 ng/mL in neat mouse serum, with intersample percent of coefficient of variability <20%, and percent nominal of control samples falling between 75% and 125% at or below the minimum required dilution of 1:80.

Gelatin-based film *in situ* zymography. Tissue cryosections were dried at room temperature and incubated in TCNB buffer with 20 μg/mL of gelatin quenched substrate (Invitrogen). GM6001 (100 μmol/L) was used as a control. After an overnight incubation at 37°C, the substrate was washed out with MilliQ water. Gelatinolytic activity appeared green on a black background.

Immunohistochemistry studies. Cryosections were fixed with ice-cold acetone, blocked with 10% goat serum and 10% BSA, and incubated with rabbit polyclonal anti-mouse (human) CD31 IgG (Abcam; 1:50). AlexaFluor 488 goat anti-human IgG (Invitrogen; 1:400) was used as a secondary antibody. Rabbit IgG (DakoCytomation) was used as a negative control.

For competition experiments, cryosections were preincubated with DX-2400 (2 μg/mL) in the presence of 100× molar excess of human recombinant MMP-14 protein (R&D Systems) or cynomolgus monkey MMP-14. Slides were incubated overnight with biotinylated DX-2400 (2 μg/mL) and then treated with streptavidin/HRP (1:200), and signals were visualized with AEC+ chromogenic substrate (DakoCytomation) and counterstained with hematoxylin (Fisher Scientific, Ltd.).

Statistical Analysis

Statistical significance of the differences was analyzed by single-factor ANOVA or Student's *t* test.

Results

Identification and characterization of a human antibody inhibitor of MMP-14. We performed phage-display library selections using the human Fab-phage library FAB310 (19) and

Published OnlineFirst February 10, 2009; DOI: 10.1158/0008-5472.CAN-08-3255

the human MMP-14-CD as a target. Approximately 1,500 individual isolates were screened on purified MMP-14-CD by protein-based ELISA, and a total of 347 MMP-14-CD binders were identified (21% hit rate). Seventy were distinct as determined by DNA sequencing, with 12 of these being found to inhibit MMP-14 activity. The Fabs all had IC_{50} values <10 nmol/L and were reformatted into hIgG1s for further characterization. Six of these IgG1s inhibited MMP-14 activity with IC_{50} values ≤5 nmol/L, with each possessing different profiles of inhibition of related MMPs. One of these antibodies, DX-2400 (IgG1κ), potently inhibited human MMP-14 (K_i = 0.8 nmol/L) following a competitive model (Fig. 1*A*). DX-2400 also inhibited mouse (K_i = 0.3 nmol/L), rat (K_i = 0.2 nmol/L), and cynomolgus monkey (K_i = 4 nmol/L) MMP-14. DX-2400 did not inhibit activity of a panel of secreted human MMPs or TACE at the highest concentration tested, 1 μmol/L, in contrast to GM6001 and Marimastat (Supplementary Table S2). In addition, DX-2400 did not inhibit the other MT-MMPs (MMP-15, MMP-16, MMP-17, and MMP-24) at concentrations up to 10 μmol/L.

MMP-14 is highly expressed in invasive cancer cell lines and endothelial cells. We first assessed the expression of MMP-14 in a number of cancer cell lines (MCF-7, MDA-MB-231, and BT-474 breast cancer cells; HT-1080 fibrosarcoma; and B16F1 melanoma cells) and endothelial cells (HUVECs) by Western blot analysis. As shown in Fig. 1*B*, the anti–MMP-14 antibody detected a major protein of 63 kDa in MDA-MB-231 cells, corresponding to proMMP-14. A specific band of 57 kDa, which represents a processed form of MMP-14 (26), was detected in MDA-MB-231, HUVECs, and HT-1080 cells. As previously shown by others (27), the poorly invasive human breast cancer cells MCF-7 lacked baseline MMP-14 protein expression even after immunoprecipitation whereas BT-474 and murine B16F1 cells showed faint bands of 63- and 57-kDa forms, respectively (data not shown).

Selective inhibition of MMP-14 activity blocks proMMP-2 processing. HT-1080 cells, which express MMP-14 and MMP-2, were used to assess the effect on MMP-2 activity by the selective inhibition of endogenous MMP-14 by DX-2400. DX-2400 blocked proMMP-2 processing, whereas a polyclonal rabbit anti–MMP-14 antibody, which does not inhibit MMP-14 activity, failed to inhibit proMMP-2 activation (Fig. 1*C*). GM6001 (K_i of 13.4 nmol/L against hMMP-14) also inhibited proMMP-2 activation but increased proMMP-9 secretion by >2.5-fold as compared with the vehicle control, whereas DX-2400 did not induce this effect (Fig. 1*C*).

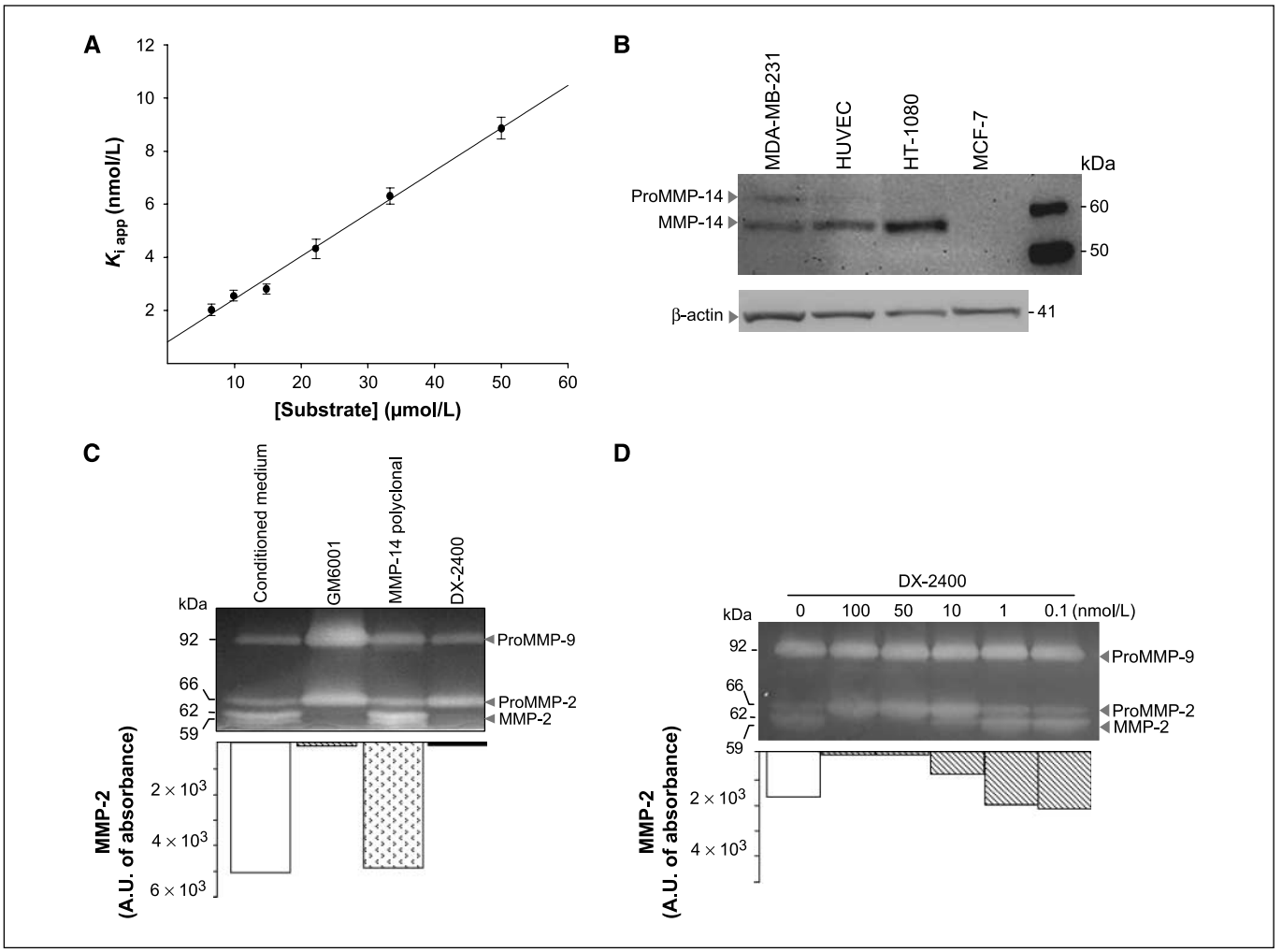

Figure 1. DX-2400 is a potent MMP-14 inhibitor that blocks proMMP-2 processing. *A,* K_i measurements for inhibition of human MMP-14. *B,* Western blot analysis. *C,* representative gelatin zymography: vehicle alone (*lane 1*), GM6001 (10 μmol/L; *lane 2*), anti–MMP-14 polyclonal antibody (67 nmol/L; *lane 3*), and DX-2400 (67 nmol/L; *lane 4*). *D,* representative gelatin zymography: vehicle alone (0) and DX-2400 (0.1–100 nmol/L). *Bottom,* quantification of the MMP-2 band intensity.

Published OnlineFirst February 10, 2009; DOI: 10.1158/0008-5472.CAN-08-3255

DX-2400 inhibited proMMP-2 activation (Fig. 1*D*) with an IC_{50} value in this assay of ~5 nmol/L. DX-2400 also reduced HT-1080 cell invasion *in vitro* by 40% to 45% (data not shown).

Selective inhibition of MMP-14 impairs migration and invasion of endothelial cells *in vitro*. DX-2400 inhibited HUVEC tube formation (IC_{50} ~6 nmol/L; Fig. 2*A*) and inhibited migration of HUVECs in a fibrin gel bead assay (60% in the presence of DX-2400 as compared with a control IgG1; Fig. 2*B*) whereas proliferation was unaffected (data not shown). DX-2400 also inhibited $VEGF_{165}$-induced invasion of HUVECs (Fig. 2*C*).

To determine whether selective inhibition of endogenous MMP-14 by DX-2400 might be responsible for blocking MMP-2 activation in endothelial cells, we assessed the presence of active forms of MMP-2 in conditioned medium of $VEGF_{165}$-stimulated HUVECs. In unstimulated endothelial cells, MMP-2 was present in its precursor and active forms (Fig. 2*D*). On $VEGF_{165}$ stimulation, the 62-kDa active MMP-2 significantly increased in intensity (Fig. 2*D*). In the presence of DX-2400, no active MMP-2 was detected in both unstimulated HUVECs and $VEGF_{165}$-stimulated HUVECs (Fig. 2*D*).

Selective inhibition of MMP-14 activity inhibits primary tumor growth in MDA-MB-231, but not MCF-7, breast cancer xenograft mouse models. We next evaluated the activity of DX-2400 in the MDA-MB-231 s.c. xenograft model. MDA-MB-231 is a highly aggressive HER2-negative human breast adenocarcinoma cell line expressing high levels of MMP-14 (Fig. 1*B*). DX-2400 monotherapy showed a dose-dependent inhibition of tumor growth (Fig. 3*A*) with the higher doses of DX-2400 (10 and 30 mg/kg) yielding tumor growth inhibitions of 76% and 70%, respectively. Doses of 1 and 3 mg/kg also showed activity in this model (48% and 59% tumor growth inhibitions). DX-2400 treatment led also to a significant reduction of tumor vascularization (CD31-staining; Fig. 3*A*, *insets*). To determine the DX-2400 concentrations necessary to elicit the direct effects on tumor cell growth in this model, we measured serum DX-2400 levels at day 10, day 20, and at study termination. Pharmacokinetic measurements made at study termination showed that DX-2400 mean serum concentrations correlated to the doses administered (Fig. 3*B*; mean serum antibody concentration of 38 ± 7, 140 ± 47, and

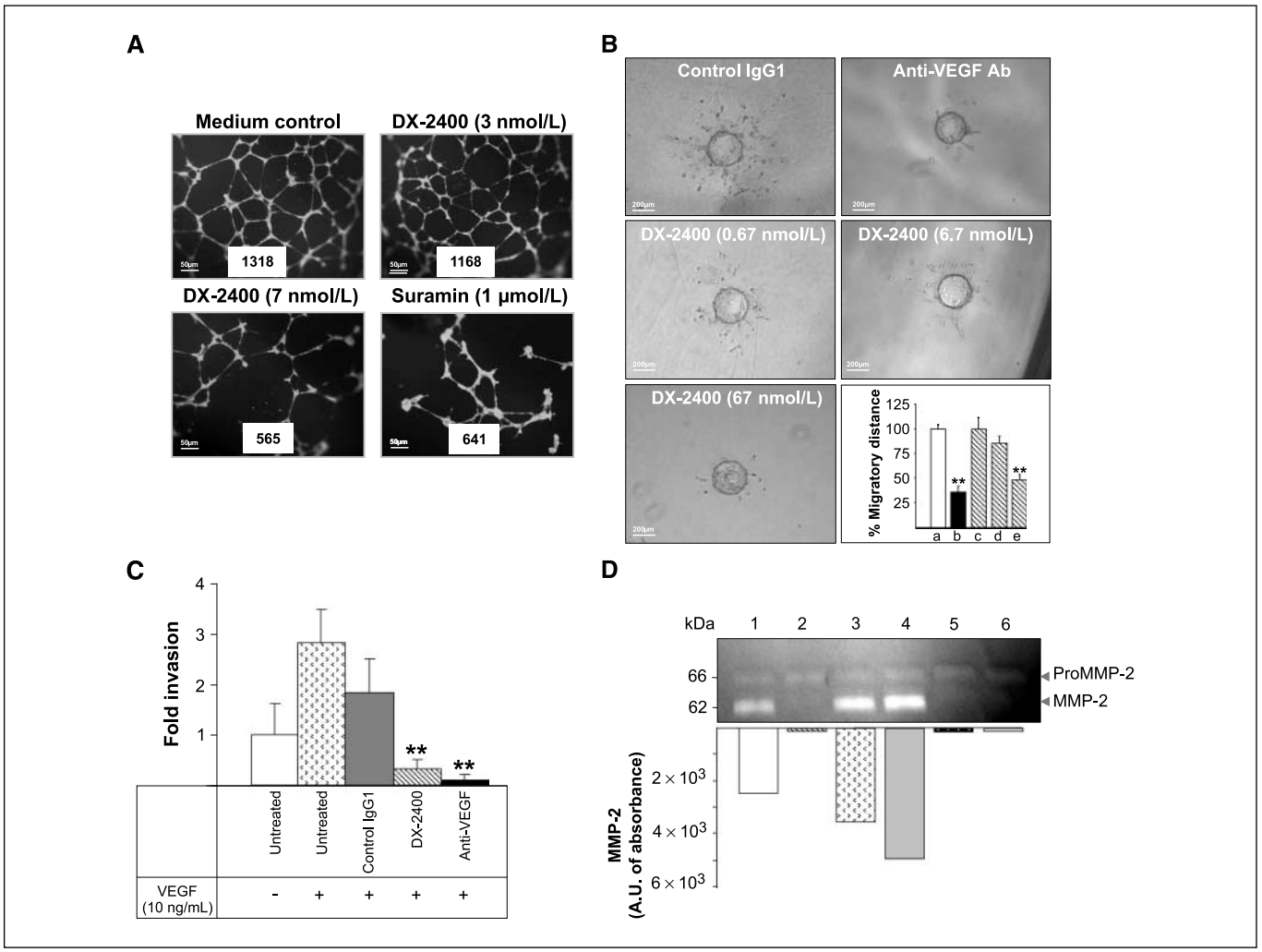

Figure 2. DX-2400 impairs invasion and migration of endothelial cells and blocks proMMP-2 processing. *A,* representative photomicrographs of the inhibitory activity of DX-2400 on HUVEC tube formation. *Bar,* 50 μm. *B,* fibrin bead assay. Representative photomicrographs of HUVEC-coated fibrin beads treated with control IgG1 (67 nmol/L), anti-VEGF antibody (67 nmol/L), and DX-2400 (0.67, 6.7, and 67 nmol/L). **, $P < 0.01$, versus control. *Columns,* mean; *bars,* SD. *Bar,* 200 μm. *C,* VEGF-induced invasion of HUVECs. **, $P < 0.01$, versus control. *Columns,* mean; *bars,* SE. *D,* representative gelatin zymography: conditioned medium alone (*lane 1*), DX-2400 6.7 nmol/L (*lane 2*), VEGF 5 ng/mL (*lane 3*), VEGF 10 ng/mL (*lane 4*), VEGF 5 ng/mL + DX-2400 6.7 nmol/L (*lane 5*), and VEGF 10 ng/mL + DX-2400 6.7 nmol/L (*lane 6*). *Bottom,* quantification of the MMP-2 band intensity. *A.U.,* arbitrary units.

Published OnlineFirst February 10, 2009; DOI: 10.1158/0008-5472.CAN-08-3255

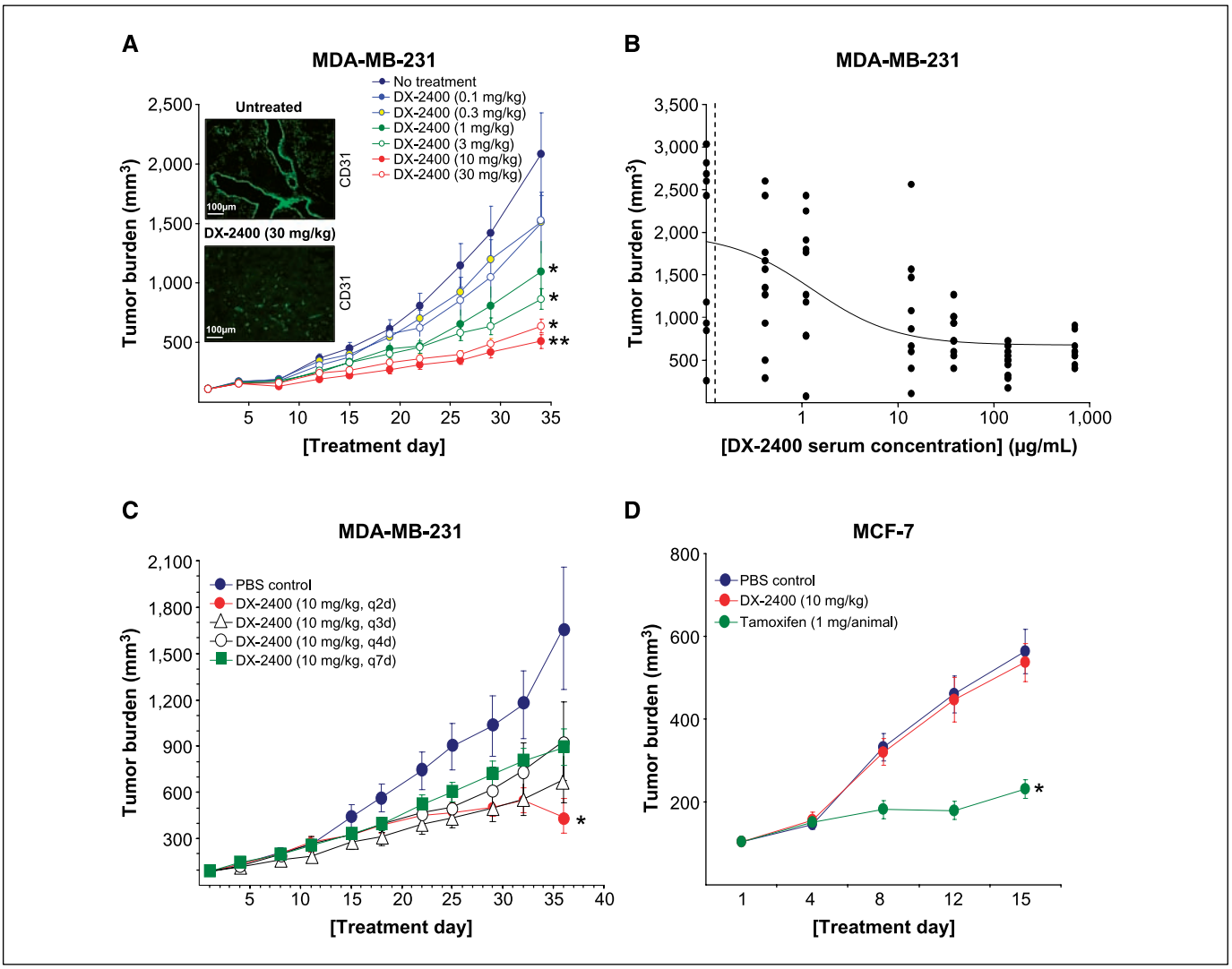

Figure 3. DX-2400 slows tumor progression in mice bearing MDA-MB-231 breast cancer xenografts. *A,* MDA-MB-231 tumor response with a dose range of DX-2400. *, $P < 0.05$; **, $P < 0.01$, versus control. *Insets,* analysis of tumoral CD31 expression in untreated and DX-2400 (30 mg/kg)–treated animals. *Bars,* 100 μm. *B,* measurement of DX-2400 concentrations in mouse serum samples as a function of tumor burden. *Dotted line,* K_i (0.12 μg/mL) for inhibition of human MMP-14 by DX-2400. *C,* frequency study. *, $P < 0.05$, versus control. *D,* MCF-7 tumor response with DX-2400 used as a single agent. *, $P < 0.05$, versus control.

697 ± 263 μg/mL for the 3, 10, and 30 mg/kg treatment groups, respectively). Similar results were observed at day 20. DX-2400 serum concentrations <110 μg/mL were measured at day 10 at the highest dose (30 mg/kg) tested. We further sought to evaluate the effect of treatment regimen on tumor growth. For this purpose, DX-2400 was administered at four different schedules. At study termination, the q2d schedule dose yielded a significant tumor growth inhibition of 73%, with the q3d, q4d, and q7d schedules also showing activity (59%, 44%, and 46% tumor growth inhibitions, respectively; Fig. 3*C*).

In contrast to MDA-MB-231 cells, MCF-7 cells do not express MMP-14 (Fig. 1*B*; ref. 27) and are poorly tumorigenic in nude mice. In addition, their capacity to develop tumors *in vivo* is not affected by tissue inhibitor of metalloproteinase-2 or batimastat (28). Consistent with the lack of MMP-14 expression in MCF-7 cells, DX-2400 failed to inhibit MCF-7 tumor xenograft growth, in contrast to tamoxifen (Fig. 3*D*).

DX-2400 significantly decreases tumoral MMP activity. We next investigated the activity of DX-2400 in an orthotopic (mammary fat pad implantation) MDA-MB-231 xenograft model. MDA-MB-231-GFP tumor–bearing animals were treated with DX-2400 for 4 weeks. Administration of DX-2400 resulted in a 75% primary tumor growth inhibition (Fig. 4*A*). We examined the expression and activity of tumoral MMPs in DX-2400–treated animals. Specifically, we measured MMP-14 expression by immunohistochemistry, total tumoral MMP activity using a peptide substrate cleavage assay, gelatinolytic activity using gelatin film-*in situ* zymography, and proMMP-2 activation using gelatin zymography. Immunohistochemical analysis showed that DX-2400 binding in DX-2400–treated tumors was significantly reduced (Fig. 4*B*), reflecting the high exposure of the tumors to our antibody. Enzymatic activity assays using a peptide substrate cleaved by a wide range of MMPs (including MMP-2 and MMP-14) on clarified supernatants extracted from tumor tissues revealed 70% less MMP activity in the tumors from DX-2400–treated animals as compared with the control IgG1-treated group (Fig. 4*C*). This inhibition reached ~90% when a high concentration of GM6001 was exogenously added. Thus, chronic

Published OnlineFirst February 10, 2009; DOI: 10.1158/0008-5472.CAN-08-3255

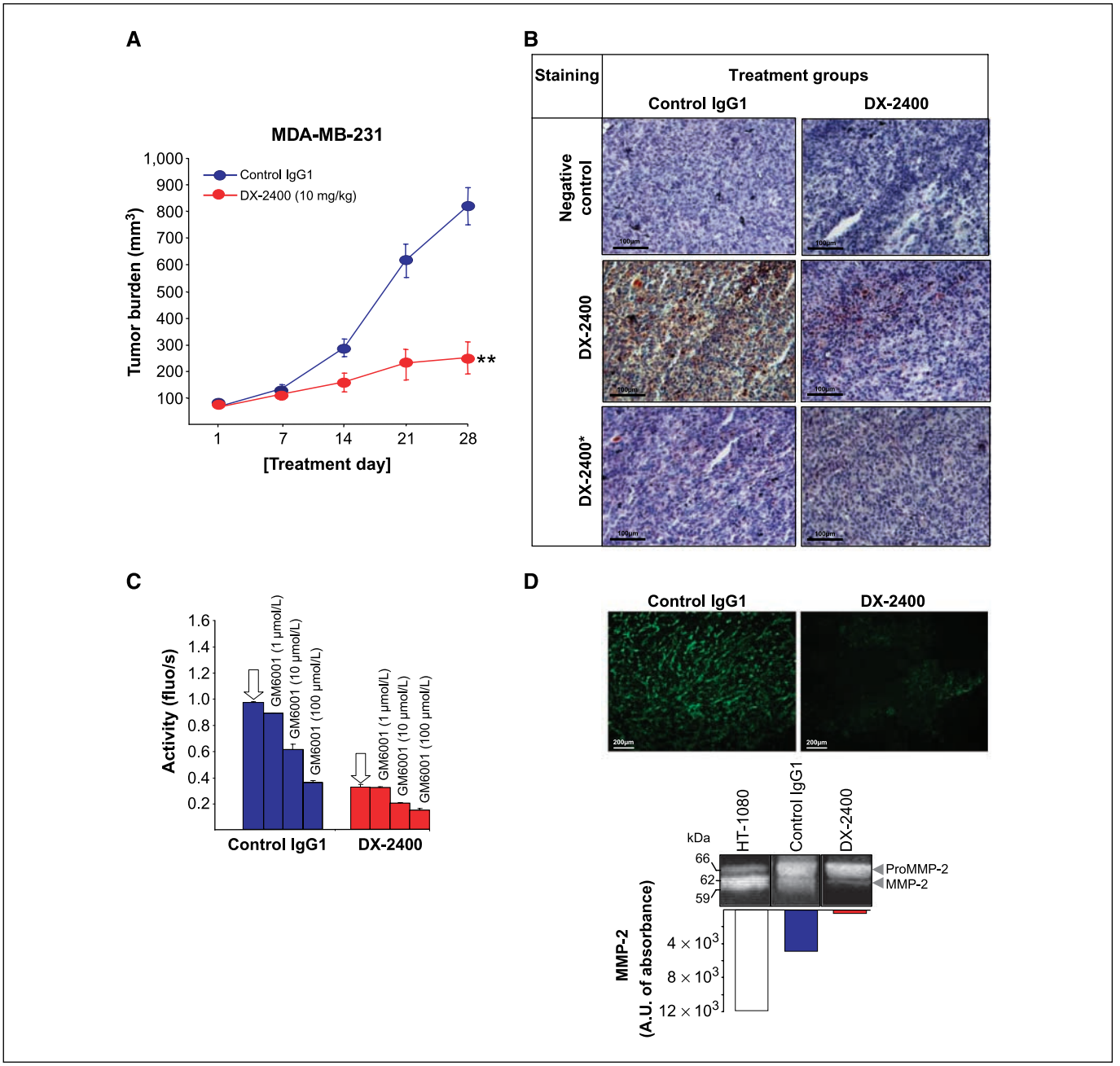

Figure 4. DX-2400 blocks tumor progression by inhibiting proteolysis in the MDA-MB-231 orthotopic model. *A,* MDA-MB-231 tumor growth curves with DX-2400 used as a single agent. **, $P < 0.01$, versus control. *B,* immunohistochemical staining with DX-2400 in control- and DX-2400–treated animals. Preincubation of tumor sections with recombinant MMP-14 abolished DX-2400 binding (*). *Bar,* 100 μm. *C,* MMP activity measurement in tumor extracts. *White arrow,* no GM6001 treatment. *D, top,* gelatin-based film *in situ* zymography on treated tumors. *Bar,* 200 μm. *Bottom,* MMP-2 activity in the tumor extracts. *Bottom,* quantification of the MMP-2 band intensity.

administration of DX-2400 significantly decreased total MMP activity in tumor tissue, and the MMP activity in MDA-MB-231-GFP tumors is largely mediated by MMP-14. Gelatin-based film *in situ* zymography on tumor sections showed a dramatic reduction of gelatinolytic activity in DX-2400–treated animals (Fig. 4*D, top*). Gelatin zymography on the tumor extracts revealed a significant reduction in active MMP-2 from DX-2400–treated animals (Fig. 4*D, bottom*), showing that the reduction of gelatinolytic activity observed by gelatin-based film *in situ* zymography in the DX-2400–treated tumors may be attributed to a reduction of MMP-2 activity.

Selective inhibition of MMP-14 activity retards metastasis. To evaluate the effect of DX-2400 on MDA-MB-231-GFP tumor metastases in the MDA-MB-231 orthotopic model, lung and liver tissues were removed at the end of the study, and the presence of GFP-positive tumor foci was assessed. Tumor-bearing animals treated with DX-2400 at the highest dose (10 mg/kg) developed significantly fewer metastatic foci in the lungs and livers as compared with animals treated with control IgG1 (Fig. 5*A*).

To investigate the direct effects of DX-2400 on pulmonary metastasis, an i.v. model was used using murine B16F1 melanoma tumor cells. In this model, tumors arise in the lung after systemic

Published OnlineFirst February 10, 2009; DOI: 10.1158/0008-5472.CAN-08-3255

extravasation following i.v. tail vein injection of tumor cells. DX-2400 treatment decreased the number of metastatic lung foci in a dose-dependent manner, reaching a maximal effect (70%) at the highest dose tested (10 mg/kg; Fig. 5*B*).

Concurrent administration of DX-2400 with paclitaxel increases tumor growth delay in the BT-474 xenograft model. We next sought to evaluate DX-2400 activity in the HER2–positive human ductal breast carcinoma model, BT-474. The purpose of this study was to evaluate the activity of DX-2400 alone or in combination with paclitaxel. BT-474 tumors in the PBS-treated group reached the 1,000 mm^3 end-point volume in a median time to end point of 33.6 days (Fig. 6*A*). Treatment of BT-474 tumor-bearing animals with paclitaxel or DX-2400 monotherapy resulted in median time to end point of 50.5 and 59.6 days, respectively, corresponding to 16.9-day (50%) and 26-day (77%) tumor growth delays. Concurrent administration of DX-2400 plus paclitaxel resulted in median time to end point of 73.3 days corresponding to 39.7 days of tumor growth delay (118%). Thus, DX-2400 showed activity against HER2–positive BT-474 tumors when used as a single agent or in combination with paclitaxel, producing a significant increase in antitumor activity in this model.

DX-2400 and bevacizumab combination increases tumor growth delay in the MDA-MB-231 xenograft model. Both bevacizumab and DX-2400 have antiangiogenic activity, but they act by different mechanisms. Bevacizumab is an anti-VEGF humanized antibody that has direct effects on endothelial proliferation through inhibition of VEGF binding and activation of VEGFR-2, whereas DX-2400 inhibits endothelial migration, in part, through a blockade of proMMP-2 activation. We evaluated the combination of DX-2400 with anti-VEGF therapy for possible augmentation of antitumor activity. The combination of DX-2400 with bevacizumab slowed tumor progression to a greater extent than did DX-2400 alone or the combination of control IgG1 with bevacizumab. Tumors from PBS- or control IgG1-treated mice reached the predefined size of 1,500 mm^3 in an average of 37.5 and 44.6 days, respectively. Bevacizumab increased the time to end point to a similar extent as DX-2400 alone (~ 18 days), whereas the

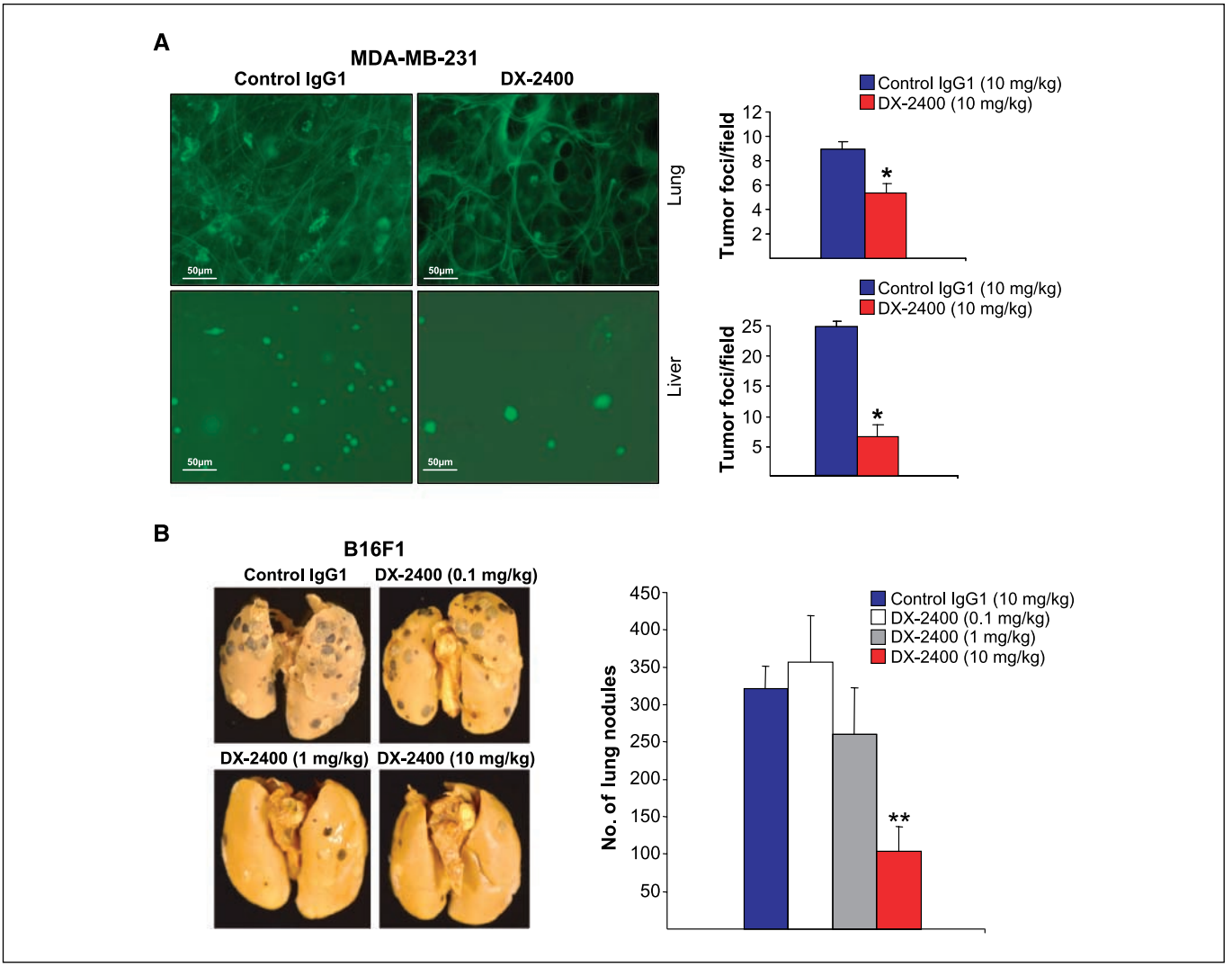

Figure 5. DX-2400 reduces the incidence of metastases in the MDA-MB-231 orthotopic model and in the i.v. mouse B16F1 melanoma model. *A,* MDA-MB-231 orthotopic model. *Left,* representative pictures of lung and liver tissues evaluated for the presence of MDA-MB-231-GFP–positive cells. *Right,* average number of tumor foci in each organ. *, $P < 0.05$, significant difference in GFP-positive cells. *Columns,* mean; *bars,* SE. *Bar,* 50 μm. *B,* B16F1 metastatic model. *Left,* representative images of lungs from control IgG1-, DX-2400 (0.1 mg/kg)–, DX-2400 (1 mg/kg)–, and DX-2400 (10 mg/kg)–treated animals. *, $P < 0.05$, significant difference in tumor foci (*right*).

Published OnlineFirst February 10, 2009; DOI: 10.1158/0008-5472.CAN-08-3255

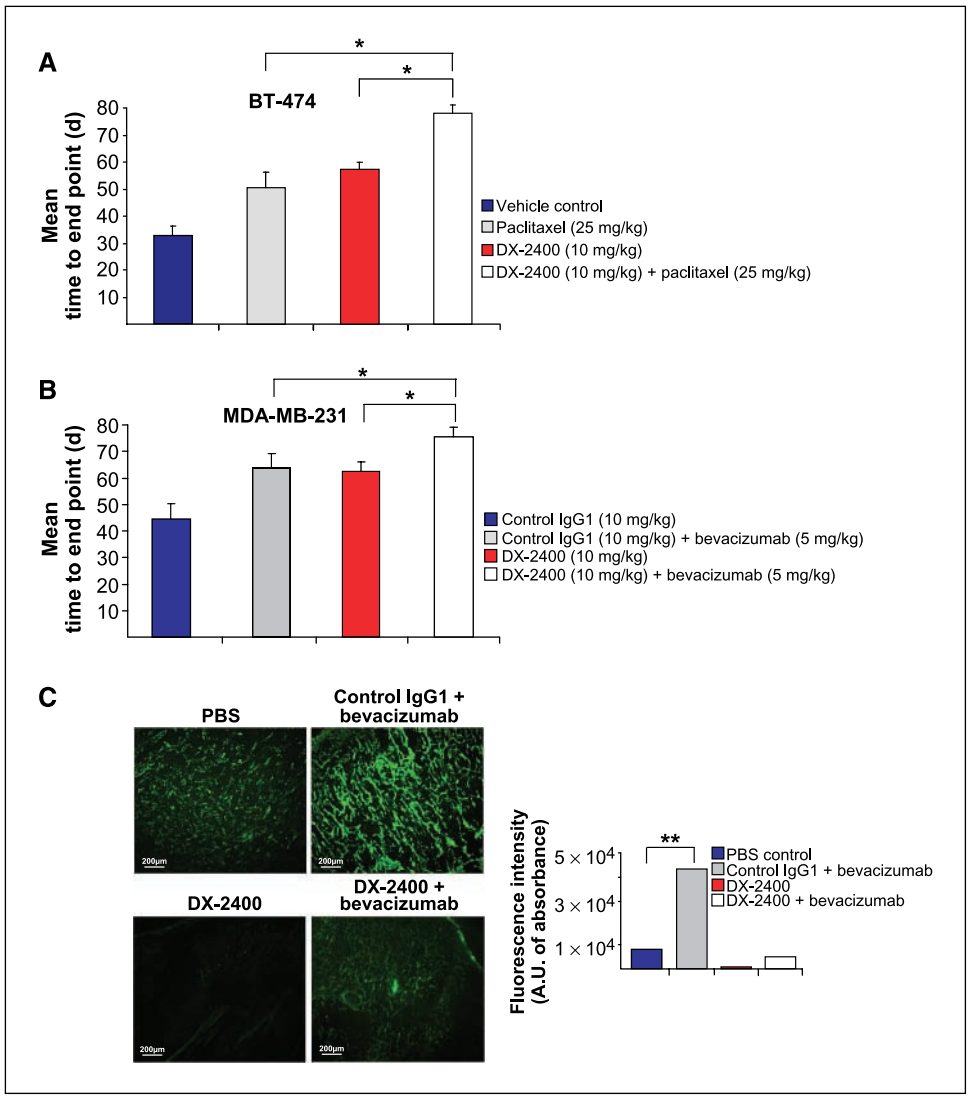

Figure 6. Combination of DX-2400 with paclitaxel or bevacizumab increases tumor growth delay in the Her-2–positive and Her-2–negative breast cancer xenograft models. *A,* determination of the time to reach the tumor end point of 1,000 mm^3 in the BT-474 tumor model. *, $P < 0.05$, versus paclitaxel monotherapy or DX-2400 monotherapy. *B,* determination of the time to reach the tumor end point of 1,500 mm^3 in the MDA-MB-231 tumor model. *, $P < 0.05$, versus bevacizumab monotherapy or DX-2400 monotherapy. *C,* gelatin-based film *in situ* zymography on MDA-MB-231–treated tumors. *Left*, representative images of tumors from PBS control, control IgG1 (10 mg/kg) + bevacizumab (5 mg/kg), DX-2400 (10 mg/kg), and DX-2400 (10 mg/kg) + bevacizumab (5 mg/kg)–treated animals. *Bars*, 20 μm. *Right,* quantification of the fluorescence intensity. **, $P < 0.01$, significant difference from PBS control–treated group.

combination of DX-2400 with bevacizumab delayed tumor growth for an additional for 13 days (Fig. 6*B*).

Gelatin-based film *in situ* zymography on MDA-MB-231 tumor sections showed a 3-fold increase of gelatinolytic activity in the tumors from bevacizumab-treated animals (Fig. 6*C*). DX-2400 completely abolished this effect, consistent with our *in vitro* findings that blocking MMP-14 activity inhibits VEGF-induced proMMP-2 activation.

Discussion

The expression of MMP-14 correlates with the malignancy of different tumor types (29, 30), and its overexpression in tumor cell lines enhances their invasiveness *in vitro* and tumorigenicity *in vivo* (5, 31). Therefore, MMP-14 is an important target for the development of a highly selective MMP inhibitor for cancer treatment.

We herein describe the identification and characterization of DX-2400, a potent and highly selective human antibody inhibitor of MMP-14 activity. DX-2400 efficiently blocked proMMP-2 activation and displayed anti-invasive activity *in vitro*. Despite their ability to block tumor cell invasion *in vitro*, some MMP inhibitors paradoxically increase MMP-9 expression (32), which could stimulate tumor formation and increase the number of liver metastases (18). Treatment of HT-1080 cells with GM6001 increased MMP-9 secretion whereas DX-2400 did not, thus showing the importance of drug specificity within the MMP family.

MMP-14 is involved during both physiologic and pathologic angiogenesis (33, 34). DX-2400 inhibited angiogenesis, in part, through inhibition of VEGF-driven cell invasion and proMMP-2 activation. The resulting antiproteolytic activity of DX-2400 may limit matrix component degradation, resulting in decreased endothelial cell invasion and angiogenesis.

Our *in vivo* studies show that DX-2400 markedly affected tumor growth of MDA-MB-231 and BT-474 tumors when used as a single agent or in combination. In contrast, this compound did not alter the growth of MCF-7 (MMP-14 negative) derived tumors, showing MMP-14 dependency for DX-2400.

In the MDA-MB-231 model, the antitumor effect of DX-2400 was associated with a strong decrease in tumor vascularization. DX-2400 treatment also induced a significant reduction of MMP activity, supporting an antiproteolytic effect of this antibody.

Published OnlineFirst February 10, 2009; DOI: 10.1158/0008-5472.CAN-08-3255

DX-2400 showed *in vivo* activity at all dosing schedules tested, with q2d schedule yielding the highest efficacy. In addition to its effects on primary tumor growth, DX-2400 also significantly reduced the number of metastatic foci *in vivo*.

DX-2400 showed activity against the HER2–positive BT-474 xenografts when used as a single agent or in combination with paclitaxel. These results make DX-2400 an attractive candidate for breast cancer patients, especially in cases where hormonal therapy and/or therapy with Herceptin (trastuzumab) is not effective. DX-2400 combined with bevacizumab resulted in increased tumor growth delay *in vivo*. This may be due to the fact that DX-2400 treatment blocks anti-VEGF antibody–stimulated increases in tumoral gelatinolytic activity. Interestingly, in gliomas anti-VEGF therapy may increase tumor invasiveness (35). Combination therapy with antiangiogenic and novel antiproteolytic agents such as DX-2400 represents a promising approach that may produce a synergistic antitumor effect and a survival benefit for patients.

Alternate approaches for the treatment of cancer are likely to be offered by the development of inhibitors selectively targeting tumor-associated MMPs while sparing other MMPs whose activity is beneficial to the host. For example, increased expression of MMP-12 by colon carcinoma cells is associated with increased survival (36) and MMP-8–deficient male mice display increased skin cancer susceptibility and delayed wound healing (37). Thus, the dual function of some MMPs during tumor progression represents an obstacle for nonselective MMP inhibitors. MMP intervention strategies (12) have met with limited clinical success and severe side effects that may be partly due to impairment of collagen turnover in the musculoskeletal system. MMP-14–deficient mice exhibit severe fibrosis of soft tissues (4). In contrast, heterozygous mice are morphologically indistinguishable from the wild-type littermates (38), suggesting that a partial inhibition of MMP-14 activity should not induce the side effects observed in the MMP-14 knockout. DX-2400 treatment of Lewis rats for 28 days at up to 75 mg/kg every 2nd day did not lead to any clinical or histologic findings including abnormalities of the joints (data not shown). These pilot toxicology study results offer the promise that DX-2400 will be well tolerated in the clinic. The pursuit of MMP-14 inhibition as a path to block tumor growth, invasion, and metastases appears attractive in light of the emerging pivotal role of MMP-14 in cancer. Our findings pharmacologically validate the role of MMP-14 in oncology and emphasize the therapeutic potential of specific antibody-based MMP inhibitors such as DX-2400.

Disclosure of Potential Conflicts of Interest

No potential conflicts of interest were disclosed.

Acknowledgments

Received 8/22/2008; revised 11/4/2008; accepted 12/3/2008.

The costs of publication of this article were defrayed in part by the payment of page charges. This article must therefore be hereby marked *advertisement* in accordance with 18 U.S.C. Section 1734 solely to indicate this fact.

We thank Arumugam Muruganandam, Rob van Hegelsom, Ed Cohen, David Buckler, Kristin Rookey, Art Ley, Jie Chen, and Mark Stochl for their support and help; Dr. Barbara Fingleton (Vanderbilt University School of Medicine) for helpful guidance and discussion; and Dr. Jerome Devy for immunohistochemical analysis.

References

1. Itoh Y, Seiki M. MT1-MMP: a potent modifier of pericellular microenvironment. J Cell Physiol 2006;206:1–8.
2. Li XY, Ota I, Yana I, Sabeh F, Weiss SJ. Molecular dissection of the structural machinery underlying the tissue-invasive activity of membrane type-1 matrix metalloproteinase. Mol Biol Cell 2008;19:3221–33.
3. Sato H, Kinoshita T, Takino T, Nakayama K, Seiki M. Activation of a recombinant membrane type 1-matrix metalloproteinase (MT1-MMP) by furin and its interaction with tissue inhibitor of metalloproteinases (TIMP)-2. FEBS Lett 1996;393:101–4.
4. Holmbeck K, Bianco P, Caterina J, et al. MT1-MMP-deficient mice develop dwarfism, osteopenia, arthritis, and connective tissue disease due to inadequate collagen turnover. Cell 1999;99:81–92.
5. Ogura S, Ohdaira T, Hozumi Y, Omoto Y, Nagai H. Metastasis-related factors expressed in pT1 pN0 breast cancer: assessment of recurrence risk. J Surg Oncol 2007;96:46–53.
6. Rozanov DV, Savinov AY, Williams R, et al. Molecular signature of MT1-MMP: transactivation of the downstream universal gene network in cancer. Cancer Res 2008;68:4086–96.
7. Tsunezuka Y, Kinoh H, Takino T, et al. Expression of membrane-type matrix metalloproteinase 1 (MT1-MMP) in tumor cells enhances pulmonary metastasis in an experimental metastasis assay. Cancer Res 1996;56:5678–83.
8. Chun TH, Sabeh F, Ota IJ, et al. MT1-MMP-dependent neovessel formation within the confines of the three-dimensional extracellular matrix. J Cell Biol 2004;167:757–67.
9. Jiang WG, Davies G, Martin TA, et al. Expression of membrane type-1 matrix metalloproteinase, MT1-MMP in human breast cancer and its impact on invasiveness of breast cancer cells. Int J Mol Med 2006;17:583–90.
10. Tetu B, Brisson J, Wang CS, et al. The influence of MMP-14, TIMP-2 and MMP-2 expression on breast cancer prognosis. Breast Cancer Res 2006;8:R28.
11. Mimori K, Ueo H, Shirasaka C, Mori M. Clinical significance of MT1-MMP mRNA expression in breast cancer. Oncol Rep 2001;8:401–3.
12. Coussens LM, Fingleton B, Matrisian LM. Matrix metalloproteinase inhibitors and cancer: trials and tribulations. Science 2002;295:2387–92.
13. Sato H. [Tumor metastasis and MMP inhibitor]. Clin Calcium 2006;16:621–6.
14. Drummond AH, Beckett P, Brown PD, et al. Preclinical and clinical studies of MMP inhibitors in cancer. Ann N Y Acad Sci 1999;878:228–35.
15. Skiles JW, Gonnella NC, Jeng AY. The design, structure, and clinical update of small molecular weight matrix metalloproteinase inhibitors. Curr Med Chem 2004;11:2911–77.
16. Egeblad M, Werb Z. New functions for the matrix metalloproteinases in cancer progression. Nat Rev Cancer 2002;2:161–74.
17. Della Porta P, Soeltl R, Krell HW, et al. Combined treatment with serine protease inhibitor aprotinin and matrix metalloproteinase inhibitor Batimastat (BB-94) does not prevent invasion of human esophageal and ovarian carcinoma cells *in vivo*. Anticancer Res 1999;19:3809–16.
18. Kruger A, Soeltl R, Sopov I, et al. Hydroxamate-type matrix metalloproteinase inhibitor batimastat promotes liver metastasis. Cancer Res 2001;61:1272–5.
19. Hoet RM, Cohen EH, Kent RB, et al. Generation of high-affinity human antibodies by combining donor-derived and synthetic complementarity-determining-region diversity. Nat Biotechnol 2005;23:344–8.
20. Jostock T, Vanhove M, Brepoels E, et al. Rapid generation of functional human IgG antibodies derived from Fab-on-phage display libraries. J Immunol Methods 2004;289:65–80.
21. Morrison JF. Kinetics of the reversible inhibition of enzyme-catalysed reactions by tight-binding inhibitors. Biochim Biophys Acta 1969;185:269–86.
22. Copeland RA. Determination of serum protein binding affinity of inhibitors from analysis of concentration-response plots in biochemical activity assays. J Pharm Sci 2000;89:1000–7.
23. Guo Y, Higazi AA, Arakelian A, et al. A peptide derived from the nonreceptor binding region of urokinase plasminogen activator (uPA) inhibits tumor progression and angiogenesis and induces tumor cell death *in vivo*. FASEB J 2000;14:1400–10.
24. Maquoi E, Frankenne F, Noel A, Krell HW, Grams F, Foidart JM. Type IV collagen induces matrix metalloproteinase 2 activation in HT1080 fibrosarcoma cells. Exp Cell Res 2000;261:348–59.
25. Mace KA, Hansen SL, Myers C, Young DM, Boudreau N. HOXA3 induces cell migration in endothelial and epithelial cells promoting angiogenesis and wound repair. J Cell Sci 2005;118:2567–77.
26. Toth M, Gervasi DC, Fridman R. Phorbol ester-induced cell surface association of matrix metalloproteinase-9 in human MCF10A breast epithelial cells. Cancer Res 1997;57:3159–67.
27. Sounni NE, Devy L, Hajitou A, et al. MT1-MMP expression promotes tumor growth and angiogenesis through an up-regulation of vascular endothelial growth factor expression. FASEB J 2002;16:555–64.
28. Noel A, Hajitou A, L'Hoir C, et al. Inhibition of stromal matrix metalloproteases: effects on breast-tumor promotion by fibroblasts. Int J Cancer 1998;76:267–73.
29. Sounni NE, Janssen M, Foidart JM, Noel A. Membrane type-1 matrix metalloproteinase and TIMP-2 in tumor angiogenesis. Matrix Biol 2003;22:55–61.
30. Van Meter TE, Broaddus WC, Rooprai HK, Pilkington GJ, Fillmore HL. Induction of membrane-type-1 matrix

Published OnlineFirst February 10, 2009; DOI: 10.1158/0008-5472.CAN-08-3255

metalloproteinase by epidermal growth factor-mediated signaling in gliomas. Neuro Oncol 2004;6:188–99.

31. Barbolina MV, Adley BP, Ariztia EV, Liu Y, Stack MS. Microenvironmental regulation of membrane type 1 matrix metalloproteinase activity in ovarian carcinoma cells via collagen-induced EGR1 expression. J Biol Chem 2007;282:4924–31.

32. Maquoi E, Sounni NE, Devy L, et al. Anti-invasive, antitumoral, and antiangiogenic efficacy of a pyrimidine-2,4,6-trione derivative, an orally active and selective matrix metalloproteinases inhibitor. Clin Cancer Res 2004;10:4038–47.

33. Basile JR, Holmbeck K, Bugge TH, Gutkind JS. MT1-MMP controls tumor-induced angiogenesis through the release of semaphorin 4D. J Biol Chem 2007;282:6899–905.

34. Arroyo AG, Genis L, Gonzalo P, Matias-Roman S, Pollan A, Galvez BG. Matrix metalloproteinases: new routes to the use of MT1-MMP as a therapeutic target in angiogenesis-related disease. Curr Pharm Des 2007;13:1787–802.

35. Chi A, Norden AD, Wen PY. Inhibition of angiogenesis and invasion in malignant gliomas. Expert Rev Anticancer Ther 2007;7:1537–60.

36. Yang X, Dong Y, Zhao J, et al. Increased expression of human macrophage metalloelastase (MMP-12) is associated with the invasion of endometrial adenocarcinoma. Pathol Res Pract 2007;203:499–505.

37. Gutierrez-Fernandez A, Inada M, Balbin M, et al. Increased inflammation delays wound healing in mice deficient in collagenase-2 (MMP-8). FASEB J 2007;21:2580–91.

38. Zhou Z, Apte SS, Soininen R, et al. Impaired endochondral ossification and angiogenesis in mice deficient in membrane-type matrix metalloproteinase I. Proc Natl Acad Sci U S A 2000;97:4052–7.

AACR American Association for Cancer Research

Cancer Research

The Journal of Cancer Research (1916–1930) | The American Journal of Cancer (1931–1940)

Selective Inhibition of Matrix Metalloproteinase-14 Blocks Tumor Growth, Invasion, and Angiogenesis

Laetitia Devy, Lili Huang, Laurent Naa, et al.

Cancer Res 2009;69:1517-1526. Published OnlineFirst February 10, 2009.